2950 Niles Road, St. Joseph, MI 49085-9659, USA
269.429.0300 fax 269.429.3852 hq@asabe.org www.asabe.org

An ASABE Meeting Presentation

Paper Number: 152181716

Anthocyanin determination in different corn hybrids using near infrared spectroscopy

Ankita A. Mangalvedhe[1], Mary-Grace C. Danao[1,*], Michael Paulsmeyer[2], Kent D. Rausch[1], Vijay Singh[1], John A. Juvik[2]

[1]Agricultural and Biological Engineering, University of Illinois, Urbana, IL 61801

[2]Crop Sciences, University of Illinois, Urbana, IL 61801

*Corresponding author: gdanao@illinois.edu

Written for presentation at the

2015 ASABE Annual International Meeting

Sponsored by ASABE

New Orleans, Louisiana

July 26 – 29, 2015

Abstract. *Anthocyanins are water soluble pigments responsible for red, blue and violet color in plant matter. They are powerful antioxidants in vitro and have shown to have anti-inflammatory and anti-carcinogenic capabilities in various laboratory studies. Many specialty corn accessions, such as maiz morado and hopi maiz, contain varying amounts of anthocyanins. The traditional approach for anthocyanin extraction and evaluation involves a series of wet chemistry techniques that are laborious and time consuming. Near infrared (NIR) spectroscopy, a more rapid technique, has been applied successfully to measure anthocyanin concentrations in berries and leaves. In this study, a high throughput assay based on NIR spectra of whole corn kernels from 950 to 1650 nm was developed for measuring anthocyanin concentration. The spectra were calibrated against total anthocyanin content (TAC) based on HPLC analysis, using partial least squares regression (PLSR). Resulting calibration models were validated with an independent set of samples. TAC of 67 specialty corn accessions ranged from 0 to 900 mg/kg. The best calibration model achieved was based on the first derivative of the entire spectral range and had coefficients of determination (R^2) of calibration and validation of 0.72 and 0.93, respectively; root mean square error of cross validation (RMSECV) of 102.16 mg/kg; ratio of standard error of prediction to reference data range (RER) of 10.9; and a ratio of standard error of performance to standard deviation (RPD) of 3.6. TAC can be estimated from the NIR spectra of whole corn kernels, which may be useful for nondestructive screening purposes.*

Keywords. *Multivariate analysis, partial least squares regression (PLSR), natural pigments, cyanidin-3-glucoside (C3G)*

Introduction

Anthocyanins are water-soluble flavonoids and polyphenolic pigments that are responsible for the red, blue and violet colors of many plants and foods (Wallace and Giusti, 2014). Interest in the anthocyanin content of foods is increasing because of their possible health benefits. Several studies show anthocyanins play a key role in scavenging free radicals, which could be used in preventing or treating chronic degenerative diseases such as atherosclerosis, aging, diabetes, hypertension, inflammation and cancer (Liu et al., 2012; Soriano Sancho and Pastore, 2012; Spormann et al., 2008; Wang and Stoner, 2008).

Structurally, anthocyanins are glycosylated 2-phenylbenzopyrilium salts (anthocyanidins). The basic structure of anthocyanidins consists of a chromane ring (C-6 – ring A and C-3 – ring C) bearing a second aromatic ring (C-6 – ring B) in position 2 (Figure 1) (Ananga et al., 2013). The various anthocyanidins differs in number and position of the hydroxyl and /or methyl ether groups attached on 3, 5, 6, 7, 3', 4' and/or 5' positions. Despite the fact that 31 different monomeric anthocyanidins have been identified, 90% of the naturally occurring anthocyanins are based on only six structures (30%, cyanidin; 22%, delphinidin; 18%, pelargonidin; and 20%, peonidin, malvidin, and petunidin) (Ananga et al., 2013).

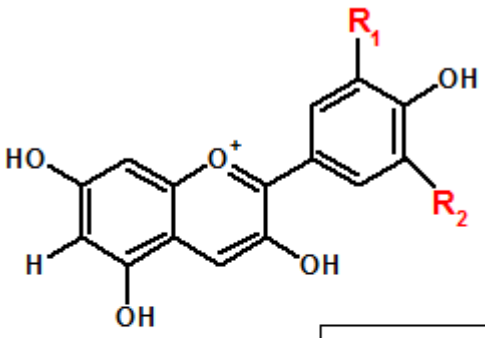

	R_1	R_2
1. Pelargonidin	H	H
2. Cyanidin	OH	H
3. Delphinidin	OH	OH
4. Peonidin	OMe	H
5. Petunidin	OMe	OH
6. Malvinidin	OMe	OMe

Figure 1. Chemical structures of six common anthocyanins. (Adapted from Ananga et al. (2013)).

Anthocyanins are commonly distributed in *Rubus* and *Vaccinium* species, strawberries, cherries, grapes, red wine, red cabbage, purple potatoes and radishes (Wallace and Giusti, 2014). Anthocyanin pigments are also found in cereal grains which vary from a simple to complex profile, depending on the number of pigments. Black and red rice grains exhibit a simple anthocyanin profile, while blue, purple and red corn varieties show a complex profile having up to 20 anthocyanin pigments (Abdel-Aal et al., 2006). Blue or purple wheat is considered to have an intermediate anthocyanin profile with four or five major anthocyanin pigments. The predominant anthocyanin compounds are cyanidin-3-glucoside (C3G) in black and red rice (Ryu et al., 1998), purple wheat (Dedio et al., 1972 and Abdel-Aal et al., 2003) and blue, purple and red corn (Abdel-Aal et al., 2006 and Moreno et al., 2005) and delphinidin-3-glucoside (D3G) in blue wheat (Abdel-Aal et al., 2006).

Several analytical methods have been used to detect and estimate anthocyanin content. These procedures include ultraviolet and visible (UV-VIS) spectroscopy (Lee and Francis, 1972), nuclear magnetic resonance (NMR) (Missang et al., 2003), mass spectrometry (MS) (Williams et al., 2002), and capillary electrophoresis (CE) (Bednár et al., 2005). While these methods are precise, they are destructive, time-consuming and costly. In addition, most of these techniques, such as NMR, require specialized reagents and personnel, which limit their application beyond the laboratory. Compared to these techniques, near infrared (NIR) spectroscopy has proved to be a fast, simple, nondestructive and chemical free analytical tool (Liu et al., 2008).

An NIR spectrum typically includes the absorbance bands of a biological sample's constituents' chemical bonds: C–H, fats, oils and carbohydrates; O–H, water and alcohol; and N–H, protein (Williams and Norris, 2001). Most absorption bands in the near infrared region are overtone or combination bands of these

fundamental absorption bands in the infrared region of the electromagnetic spectrum, which are due to vibrational and rotational transitions. The overtones and combination tones are most often affected by hydrogen bond formation (Williams and Norris, 2001).

NIR spectral data may be collected under reflectance, transmission, and transreflectance modes. In the reflectance mode, light interacts with the material and re-radiates diffuse reflected energy back into the plane of illumination. In the transmission mode, light passes through a clear or transparent sample and energy is absorbed by the chemical components. The light is not deflected as it passes through the sample. Transreflectance mode is a combination of reflectance and transmission; light reflects off the surface as it gets transmitted to the other side of the sample. Reflectance spectra are predominantly collected for ground and solid samples. Transmission spectra are collected for liquids and films. Transreflectance spectra are useful to characterize thick samples such as seeds and slurries (Williams and Norris, 2001). Both reflectance and transmittance measurements allow the simultaneous determination of multiple constituents in a sample and are commonly used to predict the composition of bulk whole grain samples in corn (Orman and Schumann, 1991). Bulk whole grain samples can be screened rapidly, require no sample preparation, and preserve the kernels after the measurement for further analysis or for propagation (Baye and Becker, 2004; Velasco et al., 1999).

With an increase in demand for natural colorants, the food and agricultural industries are looking into various anthocyanin sources. Anthocyanin pigments are located in certain layers of the cereal grain kernel. In wheat, the blue pigments are located in the aleurone layer, whereas the purple pigments are concentrated in the pericarp layers (Abdel-Aal et al., 1999). The highest concentration of anthocyanin pigments in corn was found in the pericarp, whereas the aleurone layer contained smaller concentrations (Moreno et al., 2005). Black rice was found to contain 3276 µg/g of total anthocyanins whereas red rice only contained 94 µg/g (Abdel-Aal et al., 2006). The concentration of anthocyanins in a large population of blue wheat lines was found to range from 35 to 507 µg/g with a mean 183 µg/g (Abdel- Aal et al., 1999). Abdel- Aal et al. (2006) reported total anthocyanin content (TAC) in blue, pink, purple and red corn, ranging from 51 µg/g to 1277 µg/g with purple corn containing the highest amount. They found that C3G was the most common anthocyanin in colored corn, except for pink corn, accounting for 51, 49, 47, and 31% in red, blue, multicolored, and purple corn, respectively.

Because of the great variability in anthocyanin content, a rapid and accurate method to measure anthocyanins in grains is needed to facilitate evaluation of a corn breeding program or assess anthocyanin contents during bioprocessing. Thus, the objectives of this study were to quantify TAC of 67 corn accessions and to develop a nondestructive, high throughput assay based on NIR spectroscopy to estimate TAC in whole corn kernels.

Materials and Methods

Corn samples and chemicals

Whole corn samples of 67 accessions were obtained from the Juvik Laboratory in the Department of Crop Sciences at the University of Illinois at Urbana-Champaign. HPLC grade acetonitrile (100% purity) was purchased from Avantor Performance Materials (Center Valley, PA, USA) and ACS reagent grade formic acid (97% purity) was purchased from Acros Organics (Pittsburgh, PA, USA). Water was purified by reverse osmosis system (Millipore Synergy 185 Water Filtration System, Alsace, France) and passed through a Millipore 0.45 µm LCR syring filter (Merck Millipore Ltd Tullagreen, Carrigtwohill, County Cork, Ireland) prior to use. Cyanidin 3-glucoside (C3G) (99.21% pure with 4.8% moisture content) was purchased from PhytoLab GmbH & Co. (Vestenbergsgreuth, Germany) and stored at -20˚C prior to use.

TAC measurement by HPLC

C3G was dissolved in water to form a stock solution of 2 mg C3G/ml. By serial dilution in formic acid, standard solutions of 1, 5, 10, 50, 100, 500, and 1000 µg/ml were prepared so the final formic acid concentration was 2% (v/v).

To determine the TAC of the corn, approximately a 5 g sample of kernels were ground to a fine powder using a coffee grinder (Figure 2). A subsample (1 g) of corn flour was transferred into a 15 ml centrifuge tube into which 5 ml of 2% (v/v) formic acid was added. The solution was purged of air with argon gas (> 99.9%). The tube was placed on a LabQuake rotator overnight and kept in the dark at room temperature. Afterwards, solutions were centrifuged (Model No. CT1004/D, Clay Adams, Becton, Dickinson and Co., Franklin Lakes, NJ, USA) for 15 min. The supernatant was poured into a syringe and filtered through a 0.45 µm filter (Model SLCR025NB, Millipore Millex-LCR, Merck KGaA, Billerica, MA, USA).

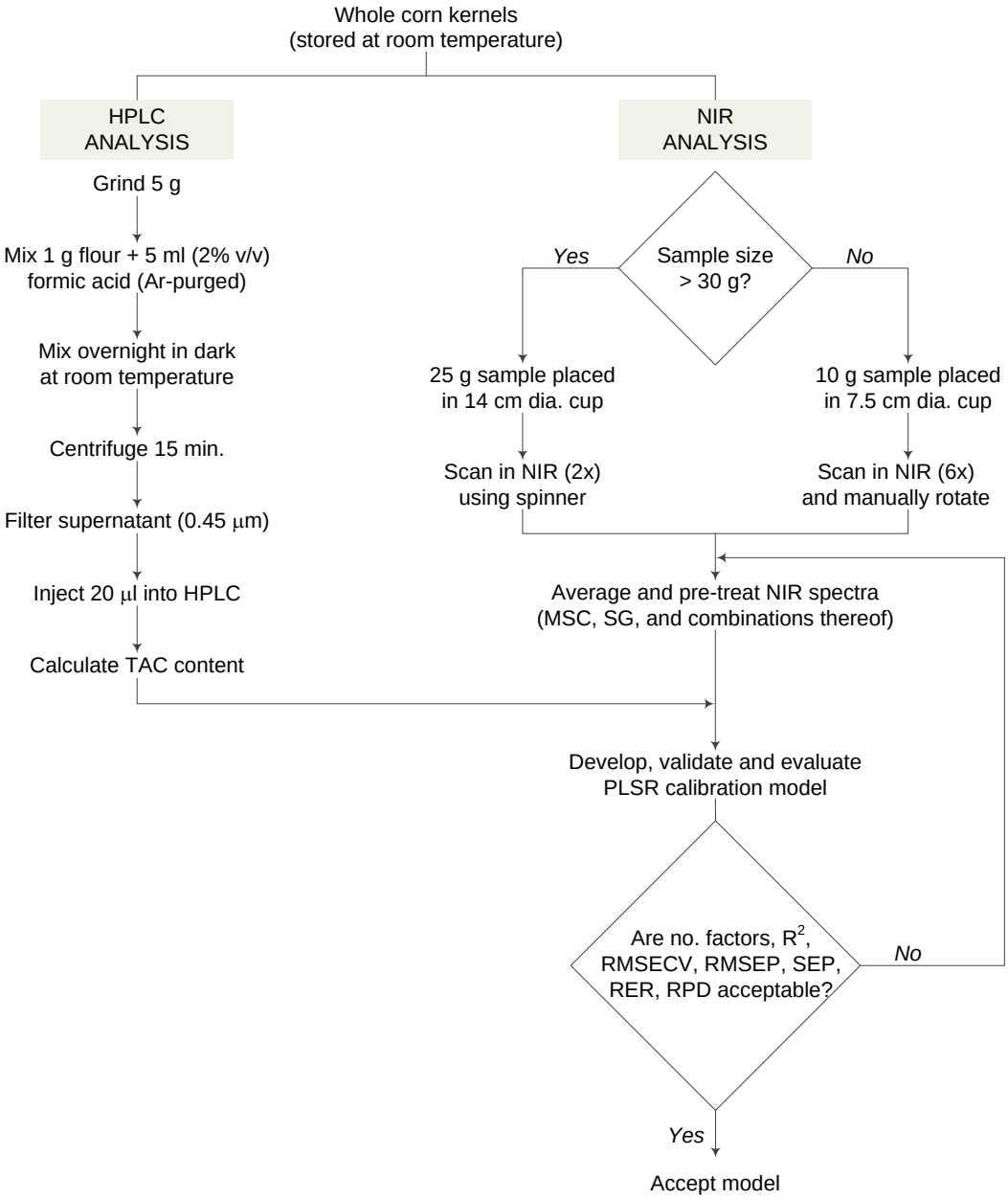

Figure 2. Analysis of corn samples for measurement of TAC by HPLC and NIR spectroscopy.

TAC analysis was performed using high-performance liquid chromatography (HPLC) on a Hitachi L-7250 (Hitachi High Technologies America Inc., Schaumburg, IL, USA) equipped with a Grace™ Alltech® Prevail™ C18 column (5μm; 4.6 x 250mm; W. R. Grace & Co., Columbia, MD, USA) maintained at 30°C. A 20 μl aliquot of each sample was injected for analysis. The mobile phase was a linear gradient of 2% formic acid (v/v) and acetonitrile beginning at 0% acetonitrile and continuing linearly to 10% acetonitrile at 3 min, then 40% acetonitrile at 30 min and back to 0% acetonitrile at 35 min. The column was eluted for 10 min after each sample with 0% acetonitrile.

C3G was used as an external standard to quantify TAC. Standard solutions were injected separately into the HPLC to generate a linear calibration curve to measure C3G content in a spreadsheet (Excel, Version 2000, Microsoft Corporation, Redmond, WA, USA) was used to generate calibration curves and to calculate final concentration.

From the HPLC, TAC was estimated in terms of μg C3G equivalents per ml using the standard calibration curve. To correct for the dilution factor of 5 ml/g whole corn powder, μg/ml were multiplied by 5 to obtain mg C3G equivalents per kg whole corn.

Collection of NIR spectra

An NIR analyzer (Model DA 7200, Perten Instruments, Hägersten, Sweden) was used to collect the spectra of whole corn kernels from 950 to 1650 nm at a resolution of 5 nm. Two types of cups were used during scanning depending on sample size. For samples greater than 30 g, approximately 25 g whole corn kernels were poured into a cup (14 cm dia.) and placed on a spinner that allowed for 180 individual spectra to be collected and averaged as the cup rotated for approximately 3 s (Figure 2). Averaging of the spectra was conducted automatically by on-board Simplicity software (Version 4.0.2.1, Simplicity Software Technologies Inc., San Bernardino, CA, USA). The sample was re-packed to collect a second averaged spectrum. An average of the two spectra was calculated in a spreadsheet (Excel, Version 2013, Microsoft Corporation, Redmond, WA, USA) and used in subsequent multivariate analysis. For samples less than 30 g, approximately 10 g whole corn kernels were poured into a second cup (7.5 cm dia.), placed in the spectrophotometer, manually rotated 60°, and scanned 180 times in between rotation. A total of 6 scans (6 x 60° = 360° rotation) for each sample was saved, averaged, and used in subsequent multivariate analysis.

Spectral processing and multivariate analysis

All spectral data were imported into Unscrambler® (Version 10.3, Camo Software, Inc., Woodbridge, NJ). The 67 corn samples were divided into a calibration set (n = 53) and a validation set (n = 14). Two preprocessing techniques were applied to the spectra: multiplicative scatter correction (MSC) or first order derivative Savitzy-Golay (SG-1) smoothing using a second order polynomial with varying number of points involved in the smoothing. The pretreated spectra were calibrated against C3G equivalents (mg/kg) using partial least squares regression (PLSR) using a non-iterative partial least squares (NIPALS) algorithm. Resulting models were first cross-validated with the calibration data set divided into 20 segments, with a minimum of two samples per segment, and then validated with the independent validation set. All models developed were evaluated on the following parameters: number of factors used in the model; coefficient of determination (R^2), root mean square errors of cross validation and prediction (RMSECV and RMSEP, respectively); ratio of performance to deviation (RPD), calculated by dividing the standard error of performance (SEP) to the standard deviation of the validation set (SD_v); and ratio of error range (RER), calculated by dividing SEP by to the range of the validation set. Models with lower RMSECV and RMSEP values are better. R^2, RPD, and RER values are typically interpreted according to guidelines in Table 1.

Table 1. Guidelines to interpretation of R^2, RPD and RER (Williams and Norris, 2001)

	Values of		Interpretation and Utility of NIR Calibration Model
R^2	RPD	RER	
Up to 0.25	0.0 – 2.3	Up to 6	Very poor, not usable
0.26 – 0.49	2.4 – 3.0	7 – 12	Poor correlation
0.50 – 0.64			OK for rough screening applications
0.66 – 0.81	3.1 – 4.9	13 – 20	Fair, OK for screening applications
0.83 – 0.90	5.0 – 6.4	21 – 30	Good, use with caution
0.92 – 0.96	6.5 – 8.0	31 – 40	Very good, use with most applications including some quality assurance
0.98 and above	8.1 and above	41 and above	Excellent, use with any application

Results and Discussion

Range of total anthocyanin content (TAC)

TAC of the 67 corn hybrids ranged from 0 to 829 mg/kg (Table 2). Yellow and orange corn samples (sample nos. 1-8) contained zero anthocyanins which was expected as these colors are attributed to the presence of lutein and zeaxanthin, which are the dominant carotenoids in these samples (Kurilich & Juvik, 1999). Several corn accessions (sample nos. 9-15) contained no detectable anthocyanin albeit being colored. This anomaly was due to variations in the flavonoid biosynthetic pathways. Tissue-specific anthocyanin production in maize requires the expression of the C1/R1 genes in the aleurone and PI1/B1 regulatory genes in the pericarp. Phlobaphenes are red pigments produced in the pericarps of some corn kernels, but their production requires only the pericarp color1 (P1) gene. P1 in these accessions produces red colored pigments called phlobaphenes instead, which accumulate in the kernel pericarp giving them a characteristic red color (Tuerck & Fromm, 1994). Two genes, Bronze1 (Bz1) and Bronze2 (Bz2), appear later in the anthocyanin biosynthetic

pathway and produce a titular bronze color when homozygous recessive. Bz1 prohibits the formation of glycosylated anthocyanins, while Bz2 prevents anthocyanins from being accumulated in the vacuoles (Cone, 2007). Anthocyanins are undetectable by the HPLC with these mutations.

Table 2. Total anthocyanin content of 67 corn hybrids.

Sample No.		TAC (mg/kg)	Sample No.		TAC (mg/kg)	Sample No.		TAC (mg/kg)
1		0	16		1.74	31		19.56
2		0	17		7.53	32		21.37
3		0	18		8.18	33		21.47
4		0	19		8.92	34		21.94
5		0	20		8.97	35		25.63
6		0	21		9.21	36		30.82
7		0	22		9.98	37		32.35
8		0	23	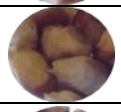	10.25	38		35.23
9	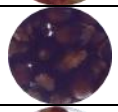	0	24		12.43	39	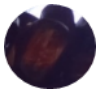	40.85
10		0	25		13.21	40		42.21
11		0	26		13.78	41		44.13
12		0	27		16.49	42		44.63
13		0	28	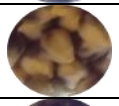	17.29	43		47.96
14	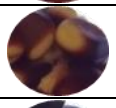	0	29		18.48	44		48.86
15		0	30		19.10	45		53.35

Table 2. Continued

Sample No.		TAC (mg/kg)	Sample No.		TAC (mg/kg)	Sample No.		TAC (mg/kg)
46		54.08	54		182.68	61	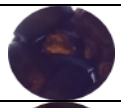	342.50
47		56.39	55		199.76	62		360.67
48		81.18	56		201.83	63		408.09
49		86.84	57		213.43	64		414.07
50		95.90	58		220.12	65		459.99
51		103.26	59		274.47	66		535.45
52		108.33	60	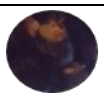	295.73	67		829.15
53		121.85						

For multivariate analysis, samples were divided into calibration and validation sets (Figure 3). TAC of samples in the calibration set ranged from 0 to 829.15 mg/kg with a mean and standard deviation of 88.93 ± 152.75 mg/kg, respectively. Likewise, TAC content of samples in the validation ranged from 0 to 535.45 mg/kg with a mean and standard deviation of 117.02 ± 177.03 mg/kg, respectively.

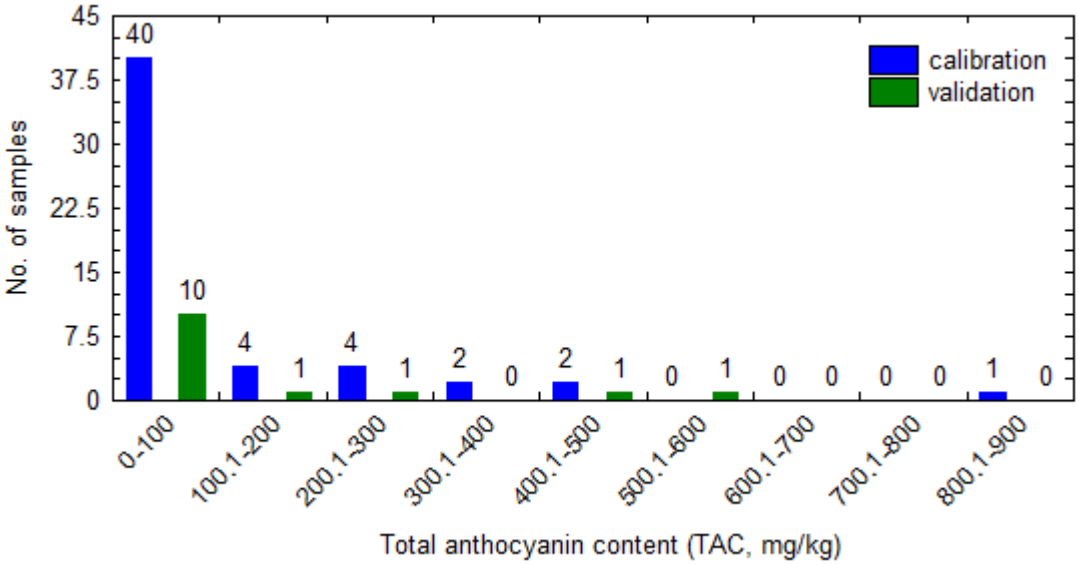

Figure 3. Histogram of calibration and validation sets used in PLSR modeling.

NIR spectral differences

The NIR spectra of whole corn kernels showed prominent peaks in the wavelength regions of 1170–1260 nm

and 1440–1560 nm, as shown in Figure 4. Peaks in the 1170–1230 nm and around 1450 nm region were associated with first overtone of C–H bonds and O–H bonds, respectively. (Cozzolino et al., 2008; Zhang et al., 2008). The peak around 1400 nm were related to the combination bands of O–H in water. Another peak around 1250 nm was due to the absorption band of the C–H stretching second overtone, which was related to the anthocyanin compounds (Chen et al., 2015). Cozzolino et al. (2008) and Zhang et al. (2008) suggested that the flavonoid constituents can be observed in the regions from 1415–1512 nm. Thus, prominent peaks in the two observed region can be associated with bands corresponding to water (first overtone of O–H stretch) and anthocyanin (C–H stretching second overtone and first and second overtone of O–H stretch) absorption.

However, these are not the only regions corresponding to flavonoid absorption. Mariani et al. (2015) found that 1232–1279, 1319–1522, 1792–2009 and 2245–2387 nm spectral regions proved to be most informative for quantification of TAC. Similarly, Cozzolino et al. (2008) suggested flavonoid constituents could be observed in regions from 1415–1512 nm, from 1650–1750 nm, and from 1955–2035 nm while Xiaowei et al. (2014) reported regions of 1677–1733 nm and 2091–2179 nm to correspond to absorption by anthocyanins.

Thus the scanning range used in this study (950–1650 nm) only partly covers the regions that correspond to absorption of anthocyanins. In order to quantify anthocyanins in these samples accurately, it is vital to scan the samples using a wider range (950–2500 nm). This will lead to incorporation of all the concerned regions, enabling development of more robust statistical models.

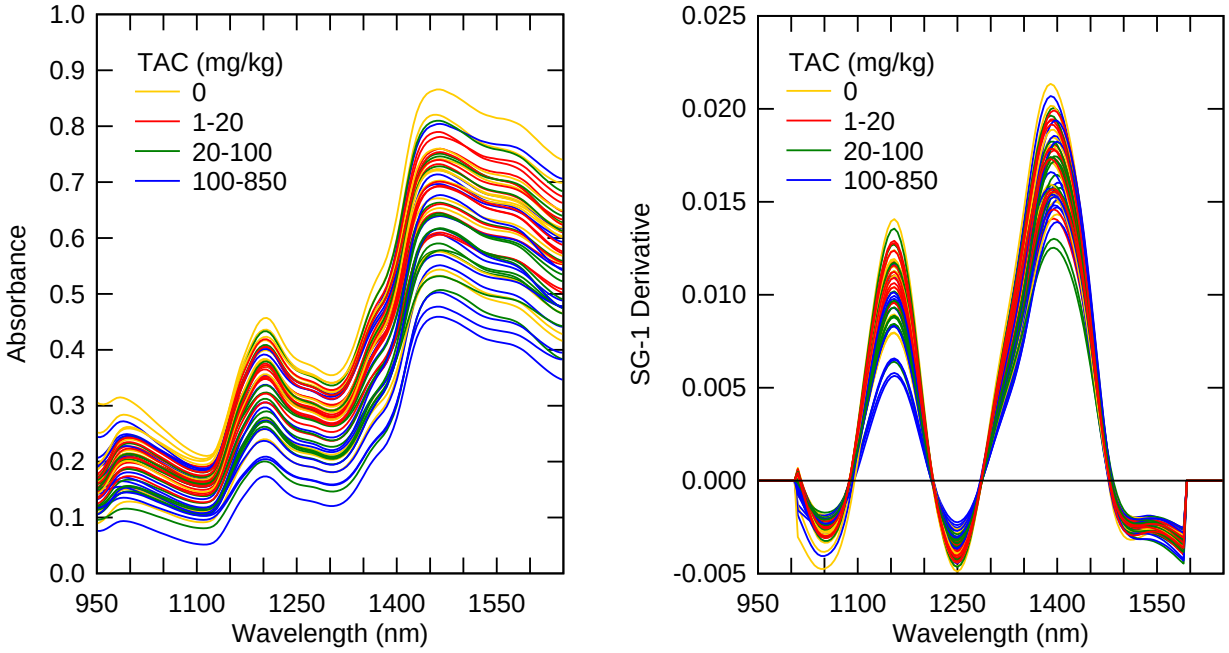

Figure 4. NIR spectra and first order Savitzky-Golay (SG-1) derivative pre-treated spectra (using 25 smoothing points) 53 corn samples used for calibration.

Predictive models and their performance

PLSR models were developed after pretreating the spectral data. The performance of PLSR models based on the entire spectral range or segments of the range are shown in Table 3. A comparison between models using the entire spectral range and selected spectral range showed that the RER and RPD values were significantly higher for the entire range. As a result, PLSR models to predict TAC concentrations using first derivative SG smoothing, MSC and their combination for preprocessing were developed for the entire range of the NIR spectra.

PLSR models based on MSC and SG pretreated spectral data had lower RER and RPD values as compared to those obtained by single first order SG pre-treatment. R^2, RER and RPD values increased with increasing number of smoothing points used in the first order SG algorithm. However, smoothing points >25 decreased these values. The best model, Model No. 8, was obtained by pretreating spectral data over the entire wavelength range with first order SG using 25 smoothing points (Figure 4). Model 8 had significantly higher correlations, R^2 (val) = 0.93, RER = 10.94 and RPD = 3.618. This model had a drawback of using six factors. Models using fewer factors had lower correlations but were still within acceptable ranges for rough screening.

Table 3. Performance of predictive PLSR models of C3G content of whole corn kernels based on NIR spectra

	Model No.									
	1	2	3	4	5	6	7	8	9	10
Spectral range (nm)	950 - 1650	950 - 1295	1295 - 1650	950 - 1650	950 - 1650	950 - 1650	950 - 1650	950 - 1650	950 - 1650	950 - 1650
Pretreatment	MSC	MSC	MSC	SG - 1	SG - 1	SG - 1	SG - 1	SG - 1	SG - 1	MSC + SG - 1
Polynomial order				2	3	2	2	2	3	2
No.of smoothing points				11	11	13	29	25	25	25
No. of factors	4	6	3	5	5	5	6	6	6	7
R^2										
calibration	0.66	0.66	0.59	0.66	0.66	0.66	0.65	0.72	0.66	0.68
validation	0.89	0.71	0.89	0.91	0.91	0.92	0.91	0.93	0.91	0.91
RMSECV (mg/kg)	120.4	129.0	117.9	118. 7	119.3	118.8	115. 9	102.2	116.7	118. 8
RMSEP (mg/kg)	61.2	104.7	73.4	59.9	65.2	57.8	57.3	50.0	64.4	58.3
SEP (mg/kg)	61.4	95.1	71.8	57.8	60.5	55.0	55.5	48.9	56.7	57.2
RER	8.71	5.63	7.46	9.27	8.86	9.73	9.65	10.94	9.44	9.37
RPD	2.88	1.86	2.47	3.06	2.93	3.22	3.19	3.62	3.12	3.09

Conclusion

This study demonstrated there is a wide range of anthocyanin concentrations across the 67 corn accessions. NIR spectra were sensitive to anthocyanin content between the 1170–1260 nm and 1440–1560 nm ranges. The best PLSR model could predict TAC with a SEP = 48.93 mg/kg. An RER = 10.94 and RPD = 3.62 indicated this model could be used for screening applications for breeding programs.

Acknowledgements

This research was supported partially by Kraft Foods Group, Inc. and by NIFA (Hatch) Project No. ILLU-731-384-"Monitoring physico-chemical changes in grain during storage." The authors thank Camo Software Inc. for providing the multivariate data analysis software, Unscrambler®, used in this study and both Ms. Jessica Bubert and Mr. Pavel Somavat for their assistance in scanning the samples.

References

Abdel-Aal, E.S.M. & Hucl, P. (1999). A rapid method for quantifying total anthocyanins in blue aleurone and purple pericarp wheats. Cereal Chem., 76(3), 350–354.

Abdel-Aal, E.S.M. & Hucl, P. (2003). Composition and stability of anthocyanins in blue-grained wheat. J. Agric. Food Chem., 51, 2174–2180.

Abdel-Aal, E.S.M., Young, J.C., & Rabalski, I. (2006). Anthocyanin composition in black, blue, pink, purple, and red cereal grains. J. Agric. Food Chem., 54 (13), 4696–4704.

Ananga, A., Georgiev, V., Ochieng, J., Phills, B., & Tsolova, V. (2013). Production of anthocyanins in grape cell cultures: a potential source of raw material for pharmaceutical, food, and cosmetic industries, The Mediterranean Genetic Code - Grapevine and Olive, Dr. Barbara Sladonja (Ed.), ISBN: 978-953-51-1067-5, InTech.

Baye, T. & Becker, H.C. (2004). Analyzing seed weight, fatty acid composition, oil, and protein contents in Vernonia galamensis germplasm by near infrared reflectance spectroscopy, JOACS, 81, 641–645.

Bednár P., Papouskova B., Müller L., Bartak P., Stávek J., Pavlousek, P., & Lemr, K. (2005). Utilization of capillary electrophoresis/mass spectrometry (CE/MSn) for the study of anthocyanin dyes. J. Sep. Sci., 28, 1291–1299.

Blanco, M. and R. González Bañó. 2003. Determination of sugars in starch hydrolysates by IR spectroscopy. *Analytical Letters* 36: 1607-1619.

Chen, S.S., Zhang, F.F., Ning, J.F., Liu, X., Zhang, Z.W., Yang, S.Q. (2015). Predicting the anthocyanin content of wine grapes by NIR hyperspectral imaging. J. Food Chem., 172, 788–793.

Cone, K.C. (2007). Anthocyanin synthesis in maize aleurone tissue. Endosperm. Columbia, MO: Springer-Verlag Berlin Heidelberg, pp. 121–139.

Cozzolino, D., Cynkar, W.U., Dambergs, R.G., Mercurio, M. D., & Smith, P.A. (2008). Measurement of condensed tannins and dry matter in red grape homogenates using near infrared spectroscopy and partial least squares. J. Agric. Food Chem., 56, 7631–7636.

Dedio, W., Hill, R. D., Evans, L. E. (1972). Anthocyanins in the pericarp and coleoptiles of purple wheat. Can. J. Plant Sci., 52, 977–980.

Delwiche, S. R. and J. B. Reeves III. 2010. A graphical method to evaluate spectral preprocessing in multivariate regression calibrations: Example with Savitzky- Golay filters and partial least squares regression. *Applied Spectroscopy* 64: 73-82.

Dykes, L., Hoffmann, L., Jr., Portillo-Ridriguez, O., Rooney, W.L., & Rooney, L.W. (2014). Prediction of total phenols, condensed tannins, and 3-deoxyanthocyanidins in sorghum grain using near-infrared (NIR) spectroscopy. J. Cereal Sci., 60, 138–142.

Foo, L. Y. and Karchesy, J. J., 1989, Chemical nature of phlopaphene. In R. W. Hemingwa and J. J. Karchesy, eds, Chemistry and Significance of Condensed Tannins (pp. 109-118). New York and London: Plenum Press.

García-Lara, S., Gutiérrez-Uribe, J.A., & Serna-Saldivar, S.O. (2012). Nutraceutical properties of blue maize. In J. C. Jimenez-Lopez (Eds.), Maize: cultivation, uses and health benefits (pp. 113–135). New York, NY: Nova Science Publishers.

Grotewold, E., Drummond, B. J., Bowen, B., and Peterson, T., 1994, The myb-homologous P gene controls phlobaphene pigmentation in maize floral organs by directly activating a flavonoid biosynthetic gene subset, Cell 76: 543-553.

Huang X., Zou X., Zhao, J., Shi, J., Zhang, X., & Holmes, M. (2014). Measurement of total anthocyanins content in flowering tea using near infrared spectroscopy combined with ant colony optimization models, J. Food Chem., 164, 536–543.

Kurilich, A.C. & Juvik, J.A. (1999). Quantification of carotenoid and tocopherol antioxidants in Zea mays. J. Agric. Food Chem., 47, 1948–1955.

Lee, D.H. & Francis, F.J. (1972). Standardization of pigment analysis in cranberries. HortScience, 7, 83–84.

Liu, Y., Chen, X., & Ouyang, A. (2008). Nondestructive determination of pear internal quality indices by visible and near-infrared spectrometry. LWT - Food Sci. Technol., 41(9), 1720–1725.

Liu, Y., Song, X., Zhang, D., Zhou, F., Wang, D., Wei, Y., & Ji, B. (2012). Blueberry anthocyanins: protection against ageing and light-induced damage in retinal pigment epithelial cells. Br. J. Nutr., 108(1), 16–27.

Mariani, N.C.T., Teixeira, G.H.A., Lima, K.M.G., Morgenstern, T.B., Nardini, V., & Cunha, L.C. (2015). NIRS and iSPA-PLS for predicting total anthocyanin content in jaboticaba fruit. J. Food Chem., 174, 643–648.

Missang, C.E., Guyot, S., & Renard, C.M.G.C. (2003). Flavonols and anthocyanins of bush butter, Dacryodes edulis (G. Don) H.J. Lam, fruit. Changes in their composition during ripening. J. Agric. Food Chem., 51, 7475–7480.

Moreno, Y.S., Sánchez, G.S., Hernández, D.R., Lobato, N.R. (2005). Characterization of antocyanin extracts from maize kernels. J. Chrom. Sci., 43, 483–487.

Murko, V.D.; Ramic, S.; Kekic, M. Die Gerbstoffe der Dalmatinischen Salvia officinalis und deren Veranderung wahrend der Lagerung. Planta Medica 25:295 (1974).

Naes, T., T. Isaksson, T. Fearn, and T. Davies, eds. 2002. *Multivariate calibration and classification*. Chichester, UK: NIR Publications.

Neves, A.C.O., Soares, G.M., De Morais, S.C., Da Costa, F.S.L., Porto, D.L., & Lima, K.M.G. (2012). Dissolution testing of isoniazid, rifampicin, pyrazinamide and ethambutol tablets using near-infrared spectroscopy (NIRS) and multivariate calibration. J. Pharm. Biomed. Anal., 57, 115–119.

Noah, L., P. Robert, S. Millar, and M. Champ. 1997. Near-infrared spectroscopy as applied to starch analysis of digestive contents. *Journal of Agricultural and Food Chemistry* 45: 2593-2597.

Orman, B.A. & Schumann, R.A. (1991). Comparison of near-infrared spectroscopy calibration methods for the prediction of protein, oil, and starch in maize grain, J. Agric. Food Chem., 39, 883–886.

Paulsen, M.R. and M. Singh. 2004. Calibration of a near-infrared transmission grain analyser for extractable starch in maize. *Biosystems Engineering* 89: 79-83.

Ryu, S. N., Park, S. Z., Ho, C.T. (1998). High performance liquid chromatographic determination of anthocyanin pigments in some varieties of black rice. J. Food Drug Anal., 6, 729–736.

Soriano Sancho, R.A. & Pastore, G M. (2012). Evaluation of the effects of anthocyanins in type 2 diabetes. Food Res. Int., 46, 378–386.

Spormann, T.M., Albert, F.W., Rath, T., Dietrich, H., Will, F., Stockis, J.-P., & Janzowski, C. (2008). Anthocyanin/polyphenolic-rich fruit juice reduces oxidative cell damage in an intervention study with patients on hemodialysis. Cancer Epidemiol Biomarkers Prevent, 17(12), 3372–3380.

Stark, E. and K. Luchter. 1986. Near-infrared analysis (NIRA): A technology for quantitative and qualitative analysis. *Applied Spectroscopy Reviews* 22: 335-399.

Styles, E. D. and Ceska, O., 1981, P and R control of flavonoids in BRONZE coleoptiles of maize, Can J Genet Cytol 23: 691-704.

Styles, E. D., and Ceska, O., 1989, Pericarp flavonoids in genetic strains of Zea mays, Maydica 34: 227-237

Tikuisis, T., D.E. Axelson, and A. Sharma. 1993. Nondestructive quantitative determination of starch content in polyethylene by solid state NMR and FTIR. *Polymer Engineering & Science* 33: 26-31.

Tuerck, J.A. & Fromm, M.E. (1994). Elements of the maize A promoter required for transactivation by the anthocyanin BICI or phlobaphene P regulatory genes. Plant Cell, 6, 1655–1663.

Velasco, L., Goffman, F.D., & Becker, H.C. (1999). Development of calibration equations to predict oil content and fatty acid composition in Brassicaceae germplasm by near-infrared reflectance spectroscopy. JAOCS, 76, 25–30.

Wallace, T.C. & Giusti, M.M. (2014). Basic anthocyanin chemistry and dietary sources. In T. C. Wallace & M. M. Giusti (Eds.), Anthocyanins in health and disease (pp. 14–89). Boca Raton, FL: CRC Press.

Wang, L.S. & Stoner, G.D. (2008). Anthocyanins and their role in cancer prevention. Cancer Lett., 269(2), 281–290.

Williams C.A., Greenham J., Harborne J.B., Kong J.M., Chia L.S., Goh N.K., Saito N., Toki K., & Tatsuzawa F. (2002). Acylated anthocyanins and flavonols from purple flowers of Dendrobium cv. ‘Pompadour. Biochem. Syst. Ecol., 30, 667–675.

Williams, P. & Norris, K. (2001). Near-Infrared Technology in the Agricultural and Food Industries, second ed. American Association of Cereal Chemists Inc., St Paul, MN.

Xiaowei, H., Xiaobo, Z., Jiewen, Z., Jiyong, S., Xiaolei, Z., Holmes, M. (2014). Measurement of total anthocyanins content in flowering tea using near infrared spectroscopy combined with ant colony optimization models. Food Chem., 164, 536–543.

Zhang, C., Shen, Y., Chen, J., Peng, X., & Bao, J. (2008). Nondestructive prediction of total phenolics, flavonoid contents, and antioxidant capacity of rice grain using near-infrared spectroscopy, J. Agric. Food Chem., 56, 8268–8272.